



## Mapping the demise of collective motion in nuclei at high excitation energy

D. Santonocito<sup>a,\*</sup>, Y. Blumenfeld<sup>b</sup>, C. Maiolino<sup>a</sup>, C. Agodi<sup>a</sup>, R. Alba<sup>a</sup>, G. Bellia<sup>a,e</sup>,  
R. Coniglione<sup>a</sup>, A. Del Zoppo<sup>a</sup>, F. Hongmei<sup>a</sup>, E. Migneco<sup>a,e</sup>, P. Piattelli<sup>a</sup>, P. Sapienza<sup>a</sup>,  
L. Auditore<sup>c,d</sup>, G. Cardella<sup>c</sup>, E. De Filippo<sup>c</sup>, E. La Guidara<sup>c</sup>, C. Monrozeau<sup>b</sup>, M. Papa<sup>c</sup>,  
S. Pirrone<sup>c</sup>, F. Rizzo<sup>a,e</sup>, A. Trifiró<sup>c,d</sup>, M. Trimarchi<sup>c,d</sup>, H.X. Huang<sup>f</sup>, O. Wieland<sup>g</sup>

<sup>a</sup> INFN – Laboratori Nazionali del Sud, via S. Sofia 62, I-95123, Catania, Italy

<sup>b</sup> Institut de Physique Nucléaire, CNRS-IN2P3, Université Paris-Sud, Université Paris-Saclay, F-91406 Orsay Cedex, France

<sup>c</sup> INFN – Sezione di Catania, via S. Sofia 64, I-95123, Catania, Italy

<sup>d</sup> INFN – Dipartimento di Scienze MIFT dell'Università di Messina, V.le F. Stagno d'Alcontres 31, I-98166, S. Agata, Messina, Italy

<sup>e</sup> Dipartimento di Fisica e Astronomia dell'Università di Catania, via S. Sofia 64, I-95123, Catania, Italy

<sup>f</sup> Key Laboratory of Science and Technology for National Defence, China Institute of Atomic Energy, P.O. Box 275(46), Beijing 102413, China

<sup>g</sup> INFN – Sezione di Milano, via Celoria 16, I-20133, Milano, Italy

### ARTICLE INFO

#### Article history:

Received 11 January 2018

Received in revised form 3 May 2018

Accepted 18 May 2018

Available online 24 May 2018

Editor: V. Metag

#### Keywords:

Giant Dipole Resonance

Hot nuclei

Fusion reactions

Statistical Model

### ABSTRACT

High energy gamma-rays from the  $^{116}\text{Sn} + ^{24}\text{Mg}$  reaction at 23A MeV were measured using the MEDEA detector at LNS – INFN Catania. Combining this new data with previous measurements yields a detailed view of the quenching of the Giant Dipole Resonance as a function of excitation energy in nuclei of mass  $A$  in the range  $120 \div 132$ . The transition towards the disappearance of the dipole strength, which occurs around 230 MeV excitation energy, appears to be remarkably sharp. Current phenomenological models give qualitative explanations for the quenching but cannot reproduce its detailed features.

© 2018 The Authors. Published by Elsevier B.V. This is an open access article under the CC BY license (<http://creativecommons.org/licenses/by/4.0/>). Funded by SCOAP<sup>3</sup>.

Studies of the Giant Dipole Resonance (GDR) built on excited states have provided a wealth of information on the dynamics of nuclei at finite temperature [1–3]. One remaining open problem in the study of the evolution of GDR properties as a function of excitation energy is the origin of the suppression of the GDR gamma yield at high excitation energies. This effect was observed, for the first time, in the study of  $^{40}\text{Ar} + ^{70}\text{Ge}$  @ 24A MeV reaction [4] where hot nuclei around 600 MeV excitation energy were populated and the gamma-ray spectrum measured in coincidence showed a sizeable strength reduction compared to standard statistical model calculations. The spectrum could be reproduced assuming an excitation energy  $E^* = 320$  MeV suggesting the interpretation of the disappearance of the GDR with increasing excitation energy and the existence of a limiting temperature for the collective motion in nuclei with mass  $A \sim 100$ .

Further evidence for the suppression of the GDR  $\gamma$  yield at very high excitation energies in the same mass region was then found by different experimental groups investigating the reactions  $^{40}\text{Ar} + ^{92}\text{Mo}$  at 21A and 26A MeV [5],  $^{36}\text{Ar} + ^{90}\text{Zr}$  at 27A MeV [6] and  $^{36}\text{Ar} + ^{98}\text{Mo}$  at 37A MeV [7] where hot nuclei were populated in an energy domain ranging from 260 to about 550 MeV. These results showed the limits of applicability of the standard statistical scenario in the description of the GDR decay from a very hot system, pointing to the need of a theoretical explanation for the quenching mechanism. A simplified approach to reproduce the gamma-ray spectra was to introduce a sharp ad hoc suppression of the gamma emission above a given excitation energy, the so called cutoff energy. In the analysis of the 27A MeV data the authors reproduced the spectra extracted at all the excitation energies using the same energy value of 250 MeV for the cutoff [8] which led the authors to conclude that  $E^*/A \sim 2.2$  MeV represents a limit for the existence of the dipole vibration for  $A \sim 110$  nuclei [8].

Different theoretical models developed to explain the GDR behaviour at high excitation energy basically follow two main ideas,

\* Corresponding author.

E-mail address: [santonocito@lns.infn.it](mailto:santonocito@lns.infn.it) (D. Santonocito).

**Table 1**

Values of the energy removed in the pre-equilibrium stage of the reaction deduced from the analysis of light charged particle energy spectra and  $E^*$  of the hot compound nucleus for all the reactions investigated.

reaction	$E_{beam}$	$E_{pre}$ (MeV)	$E^*$ (MeV)
$^{116}\text{Sn} + ^{12}\text{C}$	17A MeV	$28 \pm 10$	$150 \pm 10$
$^{116}\text{Sn} + ^{12}\text{C}$	23A MeV	$52 \pm 10$	$190 \pm 10$
$^{116}\text{Sn} + ^{24}\text{Mg}$	17A MeV	$50 \pm 20$	$270 \pm 20$
$^{116}\text{Sn} + ^{24}\text{Mg}$	23A MeV	$97 \pm 20$	$330 \pm 20$

either a suppression of the GDR [9,10] or a rapid increase of the width [11–13]. The comparison of measured gamma-ray spectra with statistical model calculations, in which the different theoretical prescriptions were implemented [8], suggested that data are better described through an approach based on GDR suppression. A similar result was obtained in the mass region  $A \sim 60 \div 70$  [14] through the study of the reaction  $^{40}\text{Ca} + ^{48}\text{Ca}$  at 25A MeV. However a clear conclusion on the quenching mechanism was never reached due to the limited agreement between data and model predictions and to the fact that the limited set of data available focused on excitation energies well above the energy at which the quenching sets in. In order to be able to draw conclusions on the GDR quenching mechanism and to delineate the energy region where the quenching appears, a complete mapping of the evolution of the GDR properties as a function of excitation energy, from a region where the GDR retains its typical features up to a region where the quenching is clearly evident, was needed.

A study of the evolution of the GDR properties as a function of excitation energy in nuclei of mass region  $A \sim 120 \div 132$  was undertaken at the Laboratori Nazionali del Sud (LNS) Catania using the MEDEA [15] multi-detector coupled to the SOLE [16,17] solenoid and the MACISTE [16,17] focal plane detector. In a first run, the reactions  $^{116}\text{Sn} + ^{12}\text{C}$  at 17A and 23A MeV, and  $^{116}\text{Sn} + ^{24}\text{Mg}$  at 17A MeV, were used to populate hot nuclei in an energy region between 150 and 270 MeV [17]. Evidence of an onset of a GDR quenching were found in the data set at  $E^* = 270$  MeV [17]. However a single energy didn't allow a study of the shape of the GDR cutoff. Therefore in a second run the reaction  $^{116}\text{Sn} + ^{24}\text{Mg}$  at 23A MeV was investigated with the same experimental setup to extend this study to higher excitation energies. Inverse kinematics were used to maximize the collection efficiency of evaporation residues on the SOLE focal plane detector. Light charged particles and gamma-rays were detected in the MEDEA detector, an array made of 180 BaF<sub>2</sub> scintillators 20 cm thick covering the polar angles from 30° to 170° degrees and the whole azimuthal angle, in coincidence with forward emitted ( $\theta < 3^\circ$ ) fusion-like residues focused by the magnetic field of SOLE solenoid on the focal plane detector MACISTE placed 16 m from the target. The time of flight of the recoils and their impact point on the focal plane detector were measured using three  $30 \times 40$  cm<sup>2</sup> low pressure MACISTE Multiwire Proportional Chambers. Three Si–Si telescopes (50  $\mu\text{m}$ –500  $\mu\text{m}$ )  $5 \times 5$  cm<sup>2</sup> each, were added on the focal plane in order to measure the Z and time of flight of the evaporation residues and to have a better control of the reaction dynamics.

Similarly to what was observed in the study of the same reaction at lower beam energy [17], the time of flight spectrum of the residues populated in the reaction  $^{116}\text{Sn} + ^{24}\text{Mg}$  at 23A MeV exhibits a broad distribution indicating the presence of complete and close to complete fusion events. A single velocity window centered around the center of mass velocity ( $V_{CM} = 5.6$  cm/ns) was chosen in order to select events with a well defined excitation energy and data analysis of light charged particle and gamma-rays was performed accordingly.

From the analysis of time of flight spectrum the mass transfer from target to projectile was evaluated. This information was com-

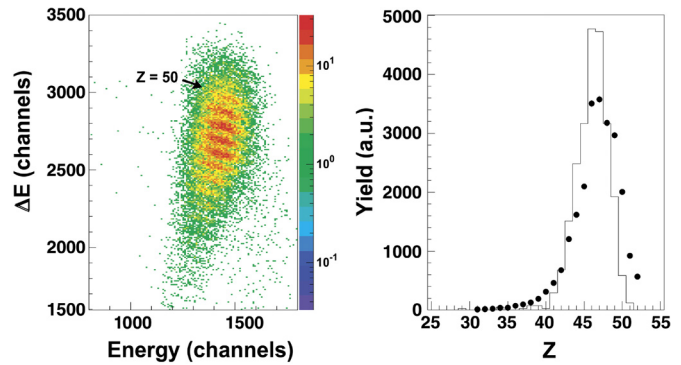


**Fig. 1.** Left) Evaporation residues  $\Delta E$ -E correlation plot measured with Si–Si telescopes placed on the SOLE focal plane. Nuclei with different Z are clearly identified. Right) Evaporation residue experimental charge distribution measured on the focal plane is shown as full symbols. GEMINI++ simulations assuming in input the same average initial excitation energy, charge and mass of the hot system populated in the reaction, filtered with spectrometer acceptance are shown for comparison as full line. (For interpretation of the colors in the figure(s), the reader is referred to the web version of this article.)

plemented with the analysis of the light charged particle energy spectra which were reproduced through a fitting procedure assuming the isotropic emission from two moving sources. This approach allowed the evaluation of the contributions coming from the equilibrated compound nucleus and pre-equilibrium emission and thus to estimate both the excitation energy and mass of the hot system populated in the reaction after the pre-equilibrium stage.

In order to deduce the excitation energy of the system a procedure similar to the one described in refs. [18,19] was undertaken. The initial momentum transfer from the projectile to the target was calculated assuming a complete fusion reaction and then the measured amount of pre-equilibrium emission, estimated from the fit of light charged particle energy spectra, was removed. Since neutrons were not detected in the experiment, the pre-equilibrium neutron multiplicity was assumed equal to the proton one. This is a reasonable assumption if the pre-equilibrium proton emission is mainly accounted for in terms of first chance  $np$  collisions [20,21] in the overlap region between colliding nuclei. This is supported by the experimental findings in this beam energy region [19,22–24]. In fact being the cross section  $\sigma_{pp} = \sigma_{nn} = 1/3\sigma_{np}$  [25],  $pp$  and  $nn$  collisions contribute less to the total amount of pre-equilibrium protons and neutrons than  $np$  collisions. In the reaction investigated the light partner is an  $N = Z$  nucleus and therefore the contributions coming from  $nn$  and  $pp$  collisions are expected to be the same. Such a scenario allows a reasonable description of both inclusive and exclusive data spanning a large range of incident energies (from 15A MeV to about 100A MeV) and projectile target combinations.

Using momentum and energy conservation the velocity, the mass and the excitation energy of the compound system can be deduced. Corrections for energy losses in the target and reaction Q-values were also taken into account. The procedure allowed to extract an excitation energy value of  $E^* = 330 \pm 20$  MeV for the hot system produced with an average mass  $A = 129$  and charge  $Z = 56$ . Errors on  $E^*$  include the error on fit parameters (temperature and multiplicity of the pre-equilibrium emitting source), and a factor of 2 indeterminacy on the estimated neutron multiplicity. The estimated values of the energy removed in the pre-equilibrium phase of the reaction and the excitation energy of the hot system are listed in Table 1 for all the reactions investigated.

The  $\Delta E$ -E correlation plot measured with the telescopes yields the Z distribution of evaporation residues focused by SOLE on the focal plane (Fig. 1a). Loci associated to residues with Z between 33 and 52 can be clearly identified. The relative yields of the evap-

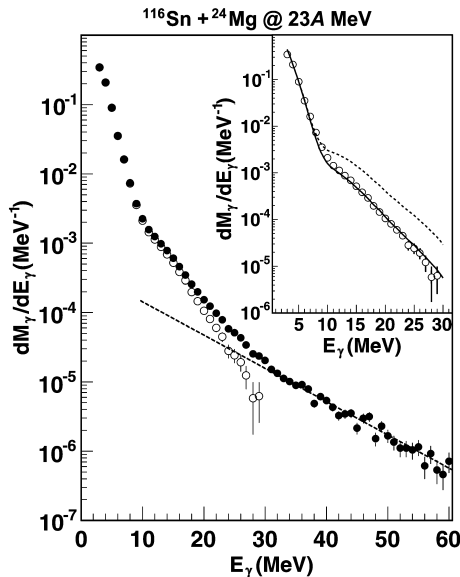


**Fig. 2.** Gamma-ray spectrum measured in the study of the reaction  $^{116}\text{Sn} + ^{24}\text{Mg}$  at 23A MeV in coincidence with evaporation residues is shown as full symbols. Dashed line corresponds to the result of fit of bremsstrahlung component extrapolated to lower energies. Statistical gamma spectrum obtained after bremsstrahlung subtraction is shown as open symbols. In the inset the same spectrum is compared with statistical model calculations. Standard statistical model calculation is shown as dashed line while a calculation assuming a sharp cutoff of the gamma-ray emission above  $E^* = 240$  MeV is shown as a full line.

oration residues as a function of their  $Z$  are shown in Fig. 1b as full symbols. As a comparison, the results of GEMINI++ [26] simulations assuming the average excitation energy, mass, charge and velocity deduced from the analysis described above, properly filtered with the spectrometer acceptance, are shown in the same figure as a full line. The GEMINI calculation, which was normalized to the integral of the experimental distribution, reproduces reasonably well the measured charge distribution in terms of centroid and width. Such a result supports the scenario of incomplete fusion accompanied by pre-equilibrium emission and, at the same time, the estimated values of average excitation energy, mass and charge of the hot system populated in the reactions. The differences observed can be explained assuming small contributions from different momentum transfer corresponding to variations in the initial excitation energy, mass and velocity of the hot nucleus populated in the reaction.

The gamma-ray spectrum measured in coincidence with fusion events is shown in Fig. 2. It was built summing over all the detectors of the rings placed around  $90^\circ$  where the Doppler shift is less than detector resolution and negligible. The spectrum displays the typical features observed when intermediate energy heavy ion collisions are used to populate hot nuclei: an exponentially decreasing component below 10 MeV associated to the statistical decay of the compound nucleus at the end of the decay chain, a bump centered around 14 MeV corresponding to the GDR decay and, above about 35 MeV a high energy tail due to bremsstrahlung radiation arising mainly from  $np$  collisions in the initial stages of the reaction.

GDR properties are typically studied through a comparison with statistical model calculations performed with the code DCASCADE [27,28]. The bremsstrahlung contribution has to be evaluated and subtracted before a proper comparison can be undertaken. A fit of the high energy part of the spectrum ( $E_\gamma > 35$  MeV) using an exponential function having slope and intensity as free parameters was performed and extrapolated to lower energies. The slope value extracted from the fit is  $9.1 \pm 0.3$  MeV, a value close to the value of  $9.5 \pm 0.3$  MeV found in the study of the reaction  $^{116}\text{Sn} + ^{12}\text{C}$  at

23A MeV [17] and coherent with the systematics of the beam energy dependence of slope parameters [29]. The result of the fitting procedure is shown in Fig. 2 as a dashed line.

The statistical gamma component obtained after bremsstrahlung subtraction is shown in Fig. 2 as open symbols. The error bars include both statistical error and the errors on the subtraction of the bremsstrahlung component connected to uncertainties on normalization and slope.

The study of the evolution of main GDR features as a function of excitation energy calls for a comparison of the statistical gamma spectrum with the results of statistical model calculations performed assuming as input the average excitation energy, mass and charge of the hot system extracted from the data analysis. A triangular spin distribution with a maximum spin leading to fusion  $J_{\text{max}} = 70\hbar$  calculated internally by the code was used, in analogy to the procedure adopted in the previous analysis of data at lower energies [17]. A Lorentzian lineshape with a centroid energy  $E_{\text{GDR}} = 14$  MeV, a width  $\Gamma_{\text{GDR}} = 13$  MeV and a strength  $S_{\text{GDR}} = 1$  corresponding to 100% of the Energy Weighted Sum Rule (EWSR) was adopted to describe the GDR. A parametrization of the level density proposed by Ormand et al. which shows a variation of the level density parameter from  $a = A/8.5$  MeV $^{-1}$  at  $T = 0$  MeV to  $a = A/12$  MeV $^{-1}$  at  $T = 5$  MeV was adopted in the calculation [30]. The choice of a level density dependent on temperature or excitation energy was motivated by the large excitation energy range to be explored in the full data set which cannot be properly described by a single level density value. Experimental values of nuclear masses, when known, were used in the code. A slightly modified version of the DCASCADE code, which includes the  $NZ/A$  dependence of GDR strength at each step of the decay process, was used in the calculation.

The calculation folded with the detector response is shown in the insert of Fig. 2 as a dashed line. While the low energy part of the spectrum is reasonably well reproduced, in the GDR region the calculation significantly overshoots the data clearly indicating the presence of a quenching phenomenon. Other statistical model calculations were performed using, as input, different choices of GDR parameters or level density parametrizations but no reasonable variation of any input parameter can explain the observed difference in the framework of the standard statistical scenario.

In order to have a quantitative evaluation of the GDR quenching, the experimental gamma spectrum and the associated DCASCADE calculation were integrated in the region from 12 to 20 MeV where the GDR yield is mainly concentrated. The gamma yields extracted in this study are compared in Fig. 3a to GDR gamma multiplicity measured in an excitation energy range between 150 and 270 MeV in nuclei in the same mass region [17]. The errors which include the statistical error, the estimated error on the bremsstrahlung subtraction and a contribution related to uncertainties in the normalization, are approximately 10% and are not visible in the figure. The experimental gamma multiplicity is observed to increase smoothly as a function of  $E^*/A$  up to about 2 MeV. Above this excitation energy value a flattening of the trend is observed and can be explained in terms of a combined effect of quenching and strength due to the different  $NZ/A$  of the hot nuclei populated in the reactions. The comparison with the results of statistical model calculations, connected by solid lines in Fig. 3a, shows that data fall below the DCASCADE predictions above  $E^*/A \approx 1.8$  MeV. Since nuclei with different average  $A$  and  $Z$  are populated in the reactions, to remove the  $NZ/A$  dependency, the ratio between experimental and calculated yields was built for each excitation energy per nucleon. Results shown in Fig. 3b indicate a progressive decrease of the ratio as a function of excitation energy per nucleon for systems above 1.5 MeV suggesting

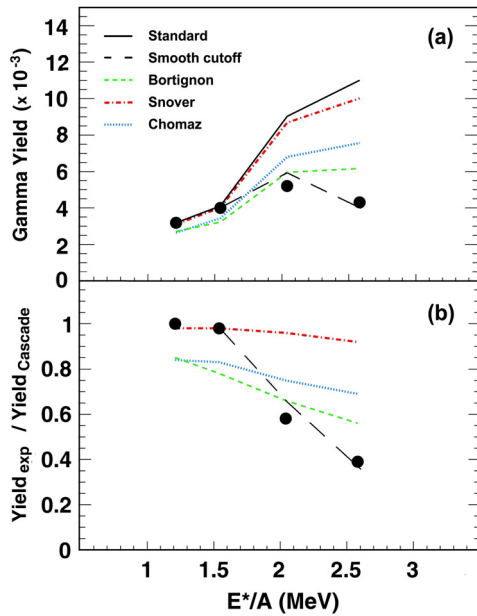


**Fig. 3.** a) GDR Gamma-ray multiplicities integrated in the region 12–20 MeV as a function of excitation energy per nucleon for the different reactions investigated. Full symbols represent the GDR  $\gamma$  multiplicity measured in the 17A MeV and 23A MeV reactions. Solid line indicate the multiplicity trend extracted from standard DCASCADE calculations relative to each reaction obtained integrating the spectra in the energy region 12–20 MeV. Green dashed, blue dotted and red dot-dashed lines represent the multiplicity trend extracted from DCASCADE calculations including respectively Bortignon, Chomaz and Snover models describing the GDR disappearance at high excitation energy. Black long dash line shows the trend extracted including a smooth cutoff of the gamma emission as described in the text. b) Ratio of the experimental GDR  $\gamma$  multiplicity to DCASCADE multiplicity shown in panel a) as a function of excitation energy per nucleon. Green dashed, blue dotted and red dot-dashed lines represent the ratio of multiplicity trend extracted from DCASCADE calculations including respectively Bortignon, Chomaz and Snover models to standard statistical model predictions. Black long dash line shows the trend extracted including a smooth cutoff of the gamma emission as described in the text.

a quenching of the GDR which seems to set in around 1.8–2 MeV excitation energy.

In the attempt to reproduce in a simple way the spectrum of the reaction  $^{116}\text{Sn} + ^{24}\text{Mg}$  at 23A MeV a sharp suppression of the gamma yield above a fixed excitation energy was introduced, similarly to what done in the study of the  $^{116}\text{Sn} + ^{24}\text{Mg}$  reaction at 17A MeV. Data were reasonably well reproduced assuming a cutoff of the gamma emission at  $E^* = 240$  MeV as shown in the insert of Fig. 2 as solid line. This value is in agreement to what was found in the analysis of the reaction  $^{116}\text{Sn} + ^{24}\text{Mg}$  at 17A MeV where a cut off value at  $E^* = 230$  MeV was used to reproduce the data. An overall coherent scenario can be depicted from these results; it points to a sudden disappearance of the GDR in nuclei for excitation energies around  $E^*/A \sim 1.7$ –1.8 MeV.

However, a sharp cutoff is clearly an oversimplification as one expects a progressive GDR disappearance. For this reason a smooth cutoff of the gamma emission as a function of excitation energy according to a Fermi function was implemented in DCASCADE. Different values of diffuseness and  $E_{cut}$ , the energy value to which the Fermi function reduces to one half, were tested in the attempt to reproduce the data set. The best agreement with data was obtained assuming a progressive suppression of the gamma emission above 200 MeV excitation energy using a value of 225 MeV for  $E_{cut}$  and of 20 MeV for the diffuseness: larger values of the diffuseness worsen the agreement. Results of these calculations are shown in Fig. 4a as a dashed line. They are very close to what has been obtained using a sharp cutoff approach but in that approach two different values of the cutoff were used to reproduce

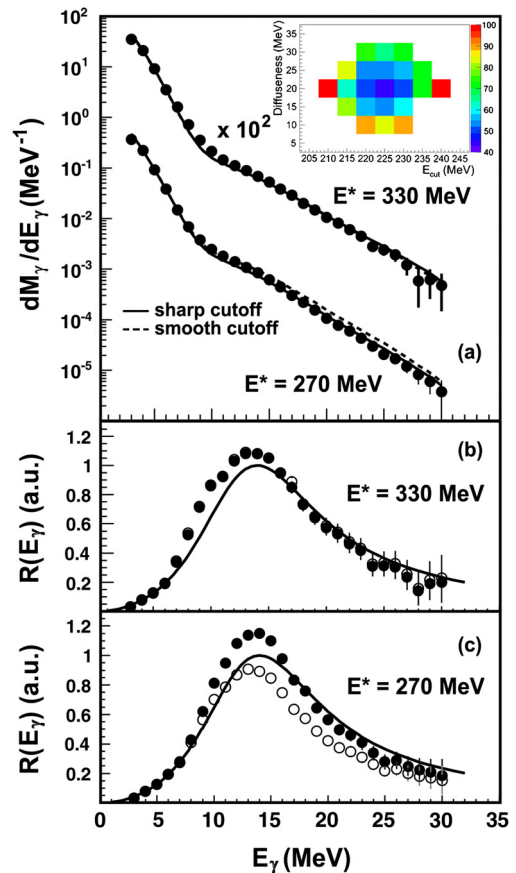


**Fig. 4.** a) Comparison between gamma spectra and statistical model calculation performed including a sharp (solid line) and a smooth (dashed line) cutoff in the gamma emission parametrized according to a Fermi function. The chi-square trend for the smooth cutoff calculations is shown in the inset. b) Comparison of the 330 MeV linearized spectra  $R(E_\gamma) = M_{\gamma\text{-exp}}/M_{\gamma\text{-CASCADE}} \times F(E_\gamma)$  and Lorentzian function  $F(E_\gamma)$  used in DCASCADE to describe the GDR arbitrarily normalized to one. Full symbols correspond to sharp cutoff calculation while open symbols correspond to smooth cutoff calculation. c) Same as b) for 270 MeV excitation energy spectra. A cutoff value at  $E^* = 230$  MeV was used in this case to better reproduce the data.

the data. The GDR gamma multiplicity obtained integrating the calculated spectra in the region from 12 to 20 MeV is shown in Fig. 3a and Fig. 3b as black long dash line. The trend obtained reproduces the high excitation energy data rather well. In order to better judge the results of the two cutoff shapes the linearized spectra  $R(E_\gamma) = M_{\gamma\text{-exp}}/M_{\gamma\text{-CASCADE}} \times F(E_\gamma)$  were built and compared to  $F(E_\gamma)$ , the Lorentzian function used in DCASCADE arbitrarily normalized to one. Fig. 4b and Fig. 4c show the results of the comparison for 330 MeV and 270 MeV excitation energy respectively. The results clearly indicate, for the first time, that GDR quenching phenomenon is rather sharp, the GDR fully disappearing in a range of about 100 MeV excitation energy.

Different theoretical models were developed to explain the GDR disappearance at high excitation energy. They can be grouped in two categories; those explaining the GDR disappearance as a real yield suppression and those interpreting the effect as due to a progressive broadening of the resonance width. Yield suppression models predict a GDR quenching based on the interplay between different time scales associated to the equilibration of collective degrees of freedom and the decay of the hot system. With increasing excitation energy the lifetime of the hot system reduces significantly and the system could start to decay by particle emission before developing a collective oscillation. Two GDR quenching factors proposed by Bortignon et al. [9] and Snover [10] were im-

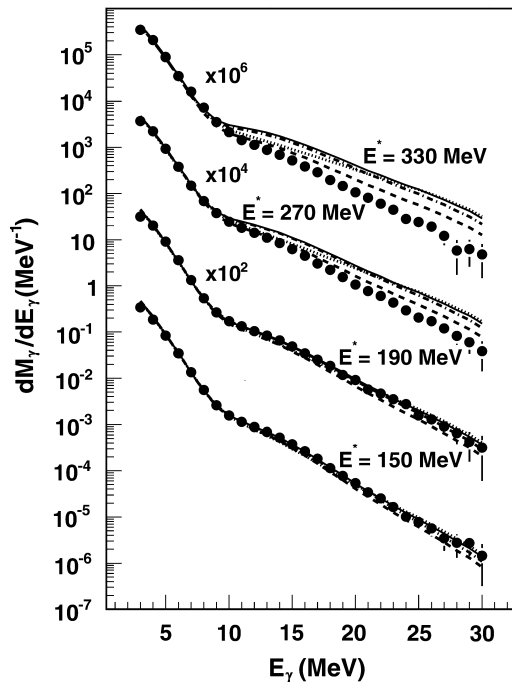


**Fig. 5.** GDR gamma spectra and associated model calculations for the full data set. Full lines correspond to standard statistical calculations, dashed lines to Bortignon model predictions, dotted lines to Chomaz model predictions and dot-dashed lines to Snover model predictions.

plemented in DCASCADE and the associated results, folded with detector response function, were compared to experimental data. The results are shown in Fig. 5 for the different excitation energies. Dashed lines show the result of the Bortignon model while dot-dashed lines show those associated to the Snover model. For comparison standard statistical model calculations are also shown as full lines. As it can be observed in the figure, the Snover approach predicts a rather soft quenching which allows to reasonably reproduce data up to 190 MeV but is not able to reproduce higher energy data, where the quenching has been observed, which are still overpredicted by calculations. The Bortignon model predicts instead a progressive quenching with excitation energy which appears in the calculation already at  $E^* = 190$  MeV where data lay above the calculation. At  $E^* = 270$  MeV the calculation reasonably reproduces the observed quenching in the data even if a slight overshoot of the data is observed. Such an effect is more evident at  $E^* = 330$  MeV where the model predictions lay well above the data. A quantitative evaluation of both model predictions is shown in Fig. 3a and Fig. 3b where the predicted gamma yields in the GDR region are compared to the full data set.

A different approach, suggested by Chomaz [13] and based on the width increase was also tested. The main idea of this approach is that each nuclear level involved in the GDR gamma decay has an intrinsic width related to its lifetime  $\tau$  according to the Heisenberg principle. This implies that transition energies between nuclear levels such as gamma-ray energies cannot be determined better than  $2\hbar/\tau$ . Assuming for each nuclear level a width  $\Gamma_{evap}$  equal to evaporation width of the hot system, the total GDR width contains the contribution of the spreading width and the nuclear levels according to the relation  $\Gamma_{GDR} = \Gamma^\downarrow + 2\Gamma_{evap}$ . Such lifetime effect was clearly observed in the study of the GDR width evolution in  $^{132}\text{Ce}$  nuclei using symmetric reactions [31]. The GDR width was observed to increase at least up to  $E^*/A = 1.5$  MeV, the highest excitation energy populated in this study. The data trend could be only reproduced including the effect of the compound nucleus

lifetime within the thermal shape fluctuation simulations [31]. Chomaz approach was also implemented as a different version of DCASCADE code and calculations were done accordingly. Results are shown as dotted lines in Fig. 5. As it can be observed from the comparison with data, this model mainly removes strength from the GDR region shifting it towards the region above 20 MeV and giving rise to a spectral shape which is not able to fit the data. The calculations suggest a quenching already at  $E^* = 190$  MeV, the comparison indicating a slight undershooting of the data in the GDR region which become progressively important with excitation energy while, above  $E_\gamma = 25$  MeV, the calculations are close or even higher than standard statistical model calculation. A more quantitative evaluation of Chomaz model predictions can be carried out from the analysis of Fig. 3a and Fig. 3b where the trend of the GDR gamma yield as a function of excitation energy per nucleon is shown as blue dotted line.

Some conclusions can be drawn from this comparison of theoretical calculations with data extracted in the mass region  $A \sim 120$ –132. The GDR quenching can be explained in terms of yield suppression and not as a progressive broadening of the width. None of the current models can fully describe the measured gamma spectra nor the very sudden quenching which is observed experimentally as a function of excitation energy. However the rather simplified approach of Bortignon et al. [9] is the one which better reproduces the overall data set. It suggests the existence of a critical temperature for the collective motion above which the nucleus would start to evaporate particles reducing its temperature before developing a collective behaviour. This affects the GDR yield which is reduced by an amount related to the time needed to develop a collective oscillation relatively to particle decay.

In summary, gamma spectra in coincidence with fusion-like residues were measured in the  $^{116}\text{Sn} + ^{24}\text{Mg}$  at 23A MeV completing a comprehensive study of the onset of quenching the GDR as a function of excitation energy. A measurement of the Z distribution of the residues gives additional confidence in the determination of the excitation energies and masses of compound nuclei. A surprisingly abrupt onset of the GDR quenching is observed which cannot be reproduced by any of the existing models. Whether this abrupt disappearance of the resonance can be related to a nuclear phase transition remains an open question. In the light of the very complete data set now available it would seem opportune to revisit this problem from a theoretical point of view.

## References

- [1] D. Santonocito, Y. Blumenfeld, *Eur. Phys. J. A* 30 (2006) 183.
- [2] M. Harakeh, A. van der Woude, *Giant Resonances: Fundamental Frequency Modes of Nuclear Excitations*, Oxford Science Publications, 2001.
- [3] P.F. Bortignon, A. Bracco, R. Broglia, *Giant Resonances: Nuclear Structure at Finite Temperature*, Harwood Academic Publishers, 1998.
- [4] J.J. Gaardhoje, et al., *Phys. Rev. Lett.* 59 (1987) 1409.
- [5] K. Yoshida, et al., *Phys. Lett. B* 245 (1990) 7.
- [6] J.H. Le Faou, et al., *Phys. Rev. Lett.* 72 (1994) 3321.
- [7] P. Piattelli, et al., *Nucl. Phys. A* 649 (1999) 181c.
- [8] T. Suomijärvi, et al., *Phys. Rev. C* 53 (1996) 2258.
- [9] P.F. Bortignon, A. Bracco, D. Brink, R.A. Broglia, *Phys. Rev. Lett.* 67 (1991) 3360.
- [10] K.A. Snover, *Nucl. Phys. A* 687 (2001) 337c.
- [11] A. Bonasera, M. Di Toro, A. Smerzi, D.M. Brink, *Nucl. Phys. A* 569 (1994) 215c.
- [12] A. Smerzi, A. Bonasera, M. Di Toro, *Phys. Rev. C* 44 (1991) 1713.
- [13] P. Chomaz, *Phys. Lett. B* 347 (1995) 1.
- [14] F. Amorini, et al., *Phys. Rev. C* 69 (2004) 014608.
- [15] E. Migneco, et al., *Nucl. Instrum. Methods Phys. Res., Sect. A* 314 (1992) 31.
- [16] G. Bellia, et al., *IEEE Trans. Nucl. Sci.* 43 (1996) 1737.
- [17] D. Santonocito, et al., *Phys. Rev. C* 90 (2014) 054603.
- [18] D. Santonocito, et al., *Phys. Rev. C* 66 (2002) 044619.
- [19] A. Chbihi, et al., *Phys. Rev. C* 43 (1991) 652.
- [20] R. Alba, et al., *Phys. Lett. B* 322 (1994) 38.
- [21] P. Sapienza, et al., *Phys. Rev. Lett.* 87 (2001) 072701.

- [22] K. Yoshida, et al., Phys. Rev. C 46 (1992) 961.
- [23] E. Holub, et al., Phys. Rev. C 28 (1983) 252.
- [24] D. Pierroutsakou, et al., Phys. Rev. C 80 (2009) 024612.
- [25] H. Nifenecker, J. Bondorf, Nucl. Phys. A 442 (1985) 478.
- [26] R.J. Charity, Phys. Rev. C 82 (2010) 014610.
- [27] F. Pulhofer, Nucl. Phys. A 280 (1977) 267.
- [28] I. Diosegi, Phys. Rev. C 64 (2001) 019801, and references therein.
- [29] Y. Schutz, et al., Nucl. Phys. A 622 (1997) 404.
- [30] W.E. Ormand, et al., Phys. Rev. C 40 (2002) 1510.
- [31] O. Wieland, et al., Phys. Rev. Lett. 97 (2006) 012501.